

## Valence and Rydberg States of FO: An ab Initio Search for Electronic Transitions

Ian C. Lane and Andrew J. Orr-Ewing\*

School of Chemistry, University of Bristol, Cantock's Close, Bristol BS8 1TS, U.K.

Received: March 8, 2000; In Final Form: July 19, 2000

An electronic absorption spectrum of FO has yet to be observed experimentally but as a guide for future spectroscopic studies of this radical, CASSCF/MRCI ab initio calculations have been performed to locate and identify the lowest energy valence and Rydberg states. No bound valence excited potentials were found save the  $a^4\Sigma^-$  state. The calculations provide estimates of the transition energies  $T_e$  to the lowest Rydberg states and the wavelengths required for spectroscopic detection. Results for both the doublet and quartet states are presented, revealing the  $3s\sigma$ ,  $3p\pi$ ,  $3p\sigma$ ,  $3d\delta$ ,  $4s\sigma$ ,  $3d\pi$ , and  $4d\delta$  Rydberg orbitals. It is likely that the repulsive valence states  $1^2\Sigma^-$  and  $1^2\Delta$  predissociate the lowest Rydberg states of the same symmetry. Consequently, the  $^2\Pi$  Rydberg states, three of which are found here, are the most promising candidates for optical detection.

## 1. Introduction

To date, there is no experimental evidence for an electronic absorption spectrum of the fluorine monoxide radical, FO. An emission spectrum in a laser-irradiated  $F_2$ /noble gas mixture has been tentatively assigned to FO,<sup>1,2</sup> but the assignment has yet to be conclusively proven. The  $A^2\Pi$  state, which is bound for the other halogen monoxides,<sup>3</sup> is calculated to be entirely repulsive for FO.<sup>2,4</sup> Rydberg states lying above the  $A^2\Pi$  continuum are candidates for spectroscopic probing of this radical and might reveal structured spectral features, but we are not aware of either vacuum ultraviolet (VUV) or resonance enhanced multiphoton ionization (REMPI)<sup>5</sup> spectra of such high-lying states. A sensitive, laser-based detection technique for this radical should prove important in, for example, kinetic studies involving fluorinated molecules relevant to atmospheric chemistry. Theoretical quantum chemistry of diatomic molecules has reached the necessary sophistication required to make quantitative determinations of the electronic potential energy curves for a radical such as FO. Ab initio calculations are reported here for the valence and low-lying Rydberg states of FO, the latter being ideal candidates for interrogation by the REMPI technique. The calculations use the complete active space self-consistent field (CASSCF) method<sup>6,7</sup> together with internally contracted multireference configurational interaction (MRCI)<sup>8</sup>, and follow a similar approach to our complementary calculations for ClO<sup>9</sup> since there are no experimental details on excited electronic states of FO to guide our choice of basis set or calculation methodology.

## 2. Overview of the Calculations

The basis sets used for the FO Rydberg calculations are summarized in Table 1 and were constructed in almost the same way as those used in our recent study of the Rydberg states of ClO.<sup>9</sup> Starting with the aug-cc-pVTZ (AVTZ) basis set of Dunning and co-workers,<sup>10</sup> successive atomic basis functions were added until a basis set adequate to describe the molecular Rydberg orbitals was achieved. One minor difference compared to ClO is that there was no need to add a tight s atomic orbital

TABLE 1: Details of the Atomic Basis Sets Used in the Calculations of the FO Rydberg States<sup>a</sup>

symmetry and multiplicity	basis set	exponents	
		F	O
all states	AVTZ +6	s: 0.027 579	s: 0.022 821
		p: 0.020 279	p: 0.016 677
		d: 0.099 724	d: 0.071 002
$2^2\Sigma^+$ , $2^2\Sigma^-$ , $4^2\Sigma^-$ , $2^2\Delta$	+ 4 more	s: 0.008 3056	s: 0.007 060 7
		s: 0.002 5013	s: 0.002 184 6
$4^2\Pi$	+ 4 more	p: 0.005 5865	p: 0.004 655 5
		p: 0.001 5390	p: 0.001 299 6
$2^2\Pi$	+ 2 more	p: 0.005 5865	p: 0.004 6555
		d: 0.034 0576	d: 0.023 557
$4^2\Sigma^+$ , $4^2\Delta$	+4 more	d: 0.011 6313	d: 0.007 8158

<sup>a</sup> All calculations required a core basis set of AVTZ + 6, with additional diffuse functions indicated above depending on the symmetries of the Rydberg states to be calculated.

to the F basis functions<sup>11</sup> as good convergence behavior is found for the first-row atoms considered here with the Dunning basis sets. The molecular Rydberg orbitals are labeled as  $n\lambda$  orbitals, where  $n$  is the principal quantum number,  $l$  is the orbital angular momentum of the Rydberg electron, and  $\lambda$  is the projection of this angular momentum on the internuclear axis. The exponents required for the additional diffuse atomic basis functions of a particular  $l$  were generated using the simple formula<sup>12</sup>

$$\alpha'(l) = \alpha(l)^2/\beta(l) \quad (1)$$

where  $\alpha'(l)$  is the new exponent required,  $\alpha(l)$  is the exponent of the most diffuse  $l$  function in the existing basis set, and  $\beta(l)$  is the exponent of the penultimate diffuse  $l$  Gaussian function. Successive application of the above formula generates ever more diffuse functions.

The aug-cc-pVTZ basis set was initially enhanced with six extra orbitals (AVTZ +6); a diffuse s, p, and d atomic orbital on each atom (see Table 1). Further functions were added depending on the angular momentum of the Rydberg electron. The basis sets were optimized by calculations of the quartet states, because these calculations demanded a larger basis set than the doublet states as more molecular Rydberg orbitals could be computed.<sup>9</sup> In addition to increasing the basis set size, the

\* Author for correspondence. Tel: +44 117 928 7672. Fax: +44 117 925 1295. E-mail: a.orr-ewing@bristol.ac.uk.

**TABLE 2: Details of the Molecular Orbital Spaces and Basis Sets Used in the FO ab Initio Calculations<sup>a</sup>**

state symmetry	active/closed orbital space	contracted/uncontracted	atomic basis set	calculation range/Å
$^4\Sigma^-$	(8220)/(2000)	2 174 750/129 131 488	AVTZ + 3s + 1p + 1d	1.22 < $R$ < 2.25
	(9220)/(3000)	5 446 880/400 506 760	AVTZ + 3s + 1p + 1d	1.22 < $R$ < 1.26
$^4\Delta$	(6222)/(2000)	2 026 708/181 456 572	AVTZ + 1s + 1p + 3d	1.22 < $R$ < 1.59
	(7221)/(2000)	2 146 234/160 575 012	AVTZ + 2s + 1p + 2d	1.46 < $R$ < 2.38
$^4\Pi$	(6430)/(2000)	6 332 985/585 575 573	AVTZ + 1s + 3p + 1d	1.26 < $R$ < 2.12
$^4\Sigma^+$	(7221)/(2000)	2 174 750/129 131 488	AVTZ + 2s + 1p + 2d	1.46 < $R$ < 2.38
$^2\Sigma^-, ^2\Sigma^+, ^2\Delta$	(8220)/(2000)	2 174 750/129 131 488	AVTZ + 3s + 1p + 1d	1.19 < $R$ < 1.32
	(6220)/(2000)	1 326 638/6 182 350	AVQZ	$R > 1.26$
$^2\Pi$	(6430)/(2000)	6 079 332/585 575 573	AVTZ + 1s + 2p + 1d	1.22 < $R$ < 1.75
	(6220)/(2000)	1 328 058/7 994 186	AVQZ	$R > 1.26$

<sup>a</sup> The first parenthetical term in the second column is the total orbital space in the CASSCF or MRCI calculation, and the second is the number of orbitals that are left closed. In both sets of parentheses, the four digits represent the number of orbitals of  $a_1$ ,  $b_2$ ,  $b_1$  and  $a_2$  symmetry, respectively. The third column details the number of contracted and uncontracted configurations generated from the CASSCF wave functions for the MRCI calculation. The exponents of the additional basis functions in the fourth column can be found in Table 1.  $R$  is the internuclear separation. Further details are in the main text.

active orbital space was also expanded to include the molecular Rydberg orbitals. As with our similar calculations on ClO, for which comparisons were possible between the calculated energies of excited states above the ground state energy and experimental spectroscopic data, the error in the relative energies is expected not to exceed  $\sim 2\%$  at  $70\,000\text{ cm}^{-1}$ . The MOLPRO 98.1 suite of programs<sup>13</sup> was used for CASSCF/MRCI level calculations, which were performed on a 16-node Beowulf system which has been described elsewhere.<sup>9</sup> The MRCI calculation in MOLPRO is limited to a maximum of five states of a particular multiplicity and symmetry. Unless specified otherwise, the computations were carried out over all the valence electrons with the core 1s orbitals frozen and the Davidson correction was applied to all MRCI energies.<sup>14</sup> Further details of the calculations specific to particular states, multiplicities, or symmetries are presented below.

### 3. Rydberg and Valence States of FO

**3.1. Quartet States of FO.** *3.1.1. Calculation Details.* The patterns of Rydberg states in the halogen oxides XO are complicated by the presence of three low-lying valence states of the ion core  $\text{XO}^+$ . The lowest quartet Rydberg states of the FO radical can only be built around the  $\text{X } ^3\Sigma^-$  ion core, whereas doublet states can also arise for the first and second excited states of the core, which have  $^1\Delta$  and  $^1\Sigma^+$  symmetry. Calculation of quartet state energies is therefore a more efficient route to map out the orderings of the lowest Rydberg orbitals.

Furthermore, because it is impossible to form a  $^4\Sigma^+$  state from the  $\text{X } ^3\Sigma^-$  ion core, the only Rydberg states (at short range) of  $^4A_1$  symmetry (MOLPRO uses  $C_{2v}$  symmetry to describe linear molecules) that can be calculated are  $^4\Delta$  states consisting of a  $d\delta$  Rydberg orbital about the  $^3\Sigma^-$  state of the ion. For calculations of the  $^4\Delta$  Rydberg states at short range, the active space employed was (6 2 2 2)/(2 0 0 0), where the first parenthetical term is the total orbital space in the CASSCF or MRCI calculation, and the second is the number of orbitals that are left closed. In both sets of parentheses, the four digits represent the number of orbitals of  $a_1$ ,  $b_2$ ,  $b_1$ , and  $a_2$  symmetry, respectively. The AVTZ + 6 basis set was further augmented by two diffuse d orbitals on each atom (see Table 1) to describe the Rydberg molecular orbitals. At intermediate bond lengths, Rydberg states with cores corresponding to the electronically excited  $A^3\Delta$  and  $A'^3\Sigma^+$  states of  $\text{FO}^+$  cross the  $nd\delta$  Rydberg states. Therefore, in this energy regime we changed the active space to (7 2 2 1)/(2 0 0 0) to include the lowest  $\sigma$  Rydberg orbital, and adjusted the basis set by removing the most diffuse d function on each atom and adding an additional s function ( $\xi$

= 0.008 305 6 on F and 0.007 060 7 on O). The calculation was limited to four states at the MRCI level.

The  $^4\Sigma^-$  states were built up from two sets of calculations using different active orbital spaces that were optimized either for calculating three Rydberg states ((9 2 2 0)/(3 0 0 0)) or the valence states ((8 2 2 0)/(2 0 0 0)). In total, five  $^4\Sigma^-$  states were calculated. Table 1 details the AVTZ + 10 basis set employed for these calculations. The  $^4\Pi$  states were calculated in a fashion similar to the corresponding states in ClO,<sup>9</sup> using three extra orbitals (two of  $b_1$  and one of  $b_2$  symmetry) to envelop the lowest two  $\pi$  Rydberg electron orbitals. For these two additional  $\pi$  molecular orbitals, two diffuse p functions on each atom were added to the AVTZ + 6 set. A total of four  $^4\Pi$  states were calculated. Table 2 contains a summary and further details about the orbital spaces and basis sets used in the calculations.

*3.1.2. Potential Curves.* The final calculated Rydberg and valence curves of the quartet states of FO are shown in Figure 1. At larger internuclear separation we see the appearance of a number of ion-pair states,<sup>15</sup> such as  $^3^4\Sigma^-$ . The emission observed in ref 1 has previously been assigned<sup>2,16</sup> to the  $^3^4\Sigma^- \rightarrow ^4^4\Sigma^-$  transition, and we find no discrepancy between our results and this conclusion. The dissociation limits of the product channels, relative to the minimum of the ground state, are listed in Table 3. Since there have been no spectroscopic determinations of any of the dissociation limits, we calculated the ground state dissociation energy ( $D_e$ ). MRCI calculations on the lowest three  $^2\Pi$  states were performed using the aug-cc-pv5z (AV5Z) basis set with the active space limited to the valence orbitals. The minimum was calculated to be  $-174.740\,172\,86$  hartrees at  $R = 1.354\,15 \pm 0.0005$  Å. To determine the dissociation energy, we calculated energy points out as far as  $R = 15$  Å. However, there is a root flip at long range between the first and second  $^2\Pi$  states which leads to a small uncertainty in the computed energy. The theoretical estimate for the ground dissociation energy is therefore  $18\,012 \pm 20\text{ cm}^{-1}$  ( $215.47 \pm 0.05\text{ kJ mol}^{-1}$ ). The stated error is the uncertainty arising solely from the effects of curtailing the calculations at  $R = 15$  Å and from the root flip at long range. It is not intended to describe the absolute accuracy of the calculation: the errors with respect to the true dissociation limit will be greater because the calculations exclude contributions from, for example, spin-orbit coupling and are not extrapolated to the complete basis set limit. Higher dissociation limits are then calculated using the known atomic energy levels,<sup>17,18</sup> ionization energies,<sup>19</sup> and electron affinities of oxygen<sup>20</sup> and fluorine.<sup>21</sup>

Figure 2a illustrates the relative energies of the Rydberg molecular orbitals as derived from the quartet calculations. The

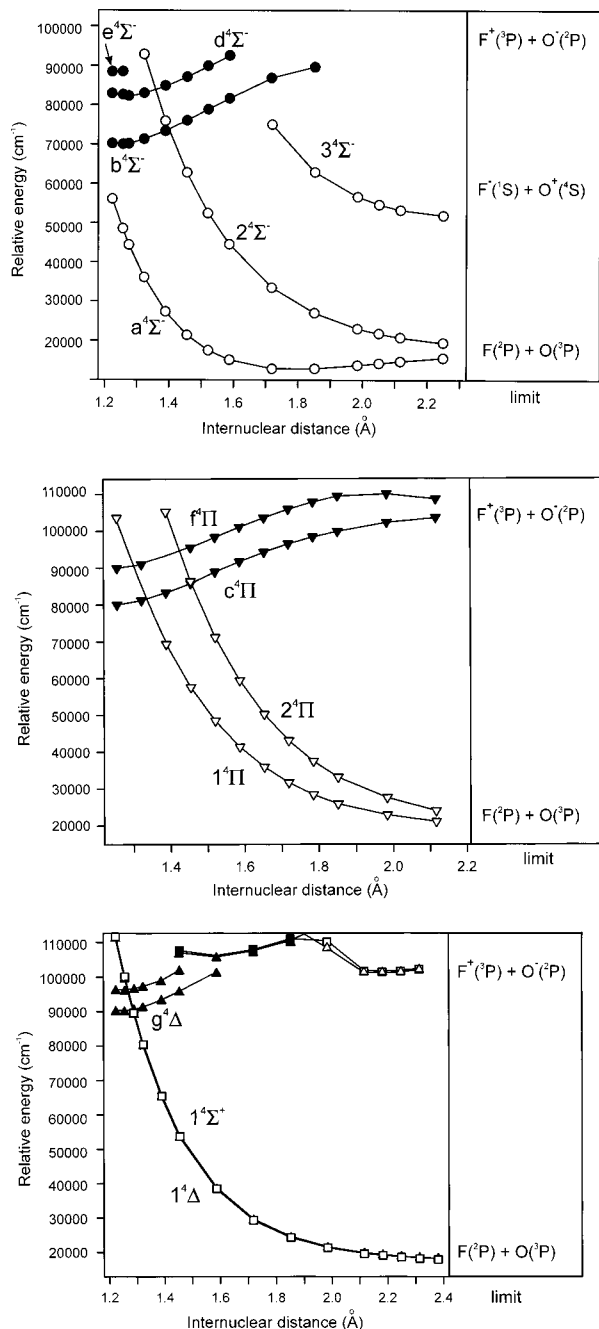


**Figure 1.** Quartet states of FO calculated using CASSCF/MRCI wave functions. The valence potentials are represented by open symbols and the Rydberg states by solids. Circles denote  $\Sigma^-$  states, squares are  $\Sigma^+$ , triangles are  $\Delta$ , and inverted triangles are  $\Pi$ . Basis set details are given in Table 1. For further details see the text. (a, top) The  $4\Sigma^-$  states. (b, middle) The  $4\Pi$  states. (c, bottom) The  $4\Delta$  and  $4\Sigma^+$  states of FO.

states labeled  $f^4\Pi$  and  $g^4\Delta$  in Figure 1 form part of the 3d complex: the analogous complex has been extensively studied in the first-row oxide NO.<sup>22,23</sup> The energy ordering of the Rydberg orbitals of FO is  $3s\sigma$ ,  $3p\pi$ ,  $3p\sigma$ ,  $4s\sigma$ ,  $3d\pi$ , and  $3d\delta$ , almost identical to that found in the doublet states of NO, which are shown for comparison in Figure 2b.<sup>23,24</sup> The minor discrepancy in the order of the  $3d\pi$  and  $3d\delta$  orbitals may be due to the small energy separation of these two orbitals (clearly demonstrated in the case of NO) perhaps exposing the small systematic error in comparing absolute energies for individual calculations of different symmetry, using their own unique basis sets, rather than using a single (large) basis set for the calculation of all the symmetry states. The separation between the three  $\lambda$

**TABLE 3: Dissociation Limits Relevant to the States Calculated in This Work<sup>a</sup>**

product channel	dissociation limit/cm <sup>-1</sup>
$F(^2P) + O(^3P)$	$18012 \pm 20$
$F(^2P) + O(^1D)$	$33974 \pm 20$
$F(^1S) + O(^4S)$	$100416 \pm 20$
$F(^2P) + O(^3P)$	$122743 \pm 20$
$F^+(^3P) + O^-(^2P)$	$146773 \pm 20$
first ionization potential	$103000 \pm 80^{29}$

<sup>a</sup> All energies are referenced to the minimum of the  $X^2\Pi$  state potential. The dissociation limits are built on a theoretical determination (CASSCF/MRCI, this work) of the dissociation energy ( $D_e$ ) of the  $X^2\Pi$  state to form  $F(^2P) + O(^3P)$  using the AV5Z basis set. Higher dissociation limits were calculated using our  $D_e$  value together with atomic transition data from refs 17 and 18, ionization data from ref 19, F electron affinity from Blondel et al. (ref 21), and electron affinity of O from Blondel (ref 20). The error of  $\pm 20$  cm<sup>-1</sup> cited for the  $D_e$  value and propagated into other table entries reflects only the uncertainties in extrapolation of our computed  $X^2\Pi$  state to infinite separation (see text for further discussion).

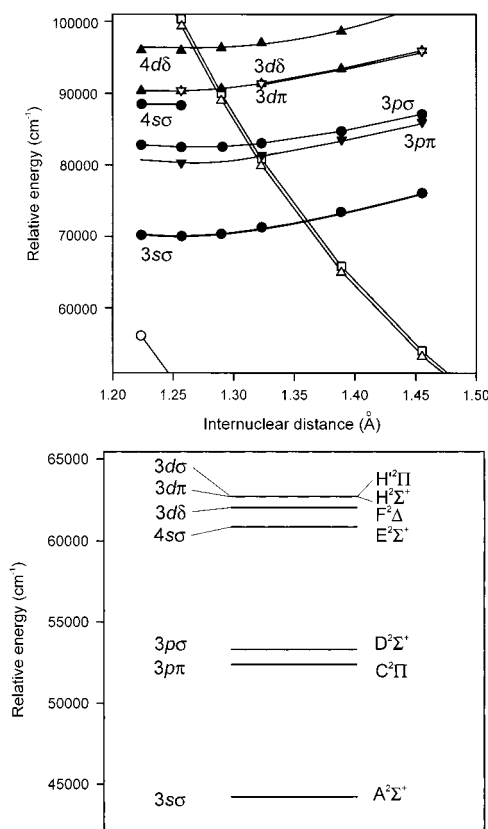


**Figure 2.** (a, top) Expanded view of the quartet Rydberg states of FO labeled according to the character of the Rydberg electron and calculated using the CASSCF/MRCI code of MOLPRO. The valence potentials are represented by open symbols, the Rydberg states by solids. Circles denote  $\Sigma^-$  states, squares are  $\Sigma^+$ , triangles are  $\Delta$ , and inverted triangles are  $\Pi$  states. The second  $4\Pi$  Rydberg state is represented by gray symbols to distinguish the potential from the neighboring  $4\Delta$  state. (b, bottom) Rydberg states of NO (from refs 23 and 24), shown for comparison.

components of the 3d complex is less than the estimated absolute energy error of our calculation (about 1500 cm<sup>-1</sup> at higher energy), though the systematic error in the relative energies of the different symmetry states should be rather less than the 2% value suspected for the energies with respect to that of the ground state. An additional  $3d\sigma$  orbital would complete the 3d complex, but could not be calculated with the present restrictions

imposed on MRCI calculations in MOLPRO. This orbital probably lies just below the  $3d\pi$  and above the  $3d\delta$  orbital.

**3.2. Doublet States of FO.** **3.2.1. Calculation Details.** As with the quartet states, the procedures for calculations of the doublet states are very similar to those used for ClO.<sup>9</sup> The basis sets for the doublet states of FO were the same as those employed in the quartet state calculations (Table 1) except for the  ${}^2\Pi$  states which used a smaller AVTZ + 8 basis set: the active space for the  ${}^2\Sigma^-$ ,  ${}^2\Sigma^+$ , and  ${}^2\Delta$  states was (8 2 2 0)/(2 0 0 0), while for the  ${}^2\Pi$  states it was (6 4 3 0)/(2 0 0 0). At short range, the modified AVTZ basis sets were necessary to ensure a good description of the Rydberg orbitals. Beyond  $R = 2.25$  bohr, however, calculations were also performed with the aug-cc-pVQZ (AVQZ) basis set, with the active space reduced to the valence orbital space alone. This alteration was made because beyond this internuclear separation the states of interest have no significant Rydberg components. A calculation performed with the AVQZ basis set has more atomic basis functions describing valence atomic orbitals, and therefore is more likely to reveal subtle features of the long-range molecular energy curves. For  $R > 2.5$  bohr, the calculations were solely performed with the AVQZ basis set and appropriate active space. A comparison of the results of calculations for  $2.25 < R < 2.5$  bohr revealed that use of the AVQZ basis set resulted in lower absolute energies than were computed with the AVTZ +  $n$  basis set. This is not surprising because calculations performed with different basis sets and active spaces will inevitably result in nonphysical differences in absolute energies of states. In the current study, however, these differences are quite small compared to the energies of the Rydberg states above the ground state.

The primary motivation in the FO calculations is not to deduce absolute energies of states, but rather to obtain the relative energies of the excited electronic states with respect to the ground state. To form continuous potential energy curves from the Rydberg state region to the dissociation limits, we computed the average energy shift for each state between the AVTZ +  $n$  and AVQZ set calculations over the range  $2.25 < R < 2.5$  bohr, and evaluated the mean of these energy shifts for eight states of different symmetry. Since the AVTZ +  $n$  basis sets should give the better descriptions of the energies of the Rydberg states above the ground state in the Franck–Condon window, we then moved all the calculated AVQZ energies (including those for repulsive valence states) by the mean energy shift, +0.033 25 hartree. Subsequent quoted energies of these excited states and derived wavelengths for spectroscopic transitions thus correspond to computations with the AVTZ +  $n$  basis set and associated active space.

**3.2.2. Potential Curves.** Calculated potential energy curves for doublet valence and Rydberg states of FO are shown in Figure 3. The valence states are all repulsive, save for the ground state. The similarity in the Rydberg orbital structure of ClO (ref 9) and FO (Figure 2a) might suggest that the doublet Rydberg states of the two radicals must also share a straightforward correspondence. However, this is not the case because the doublet states arise from the  ${}^3\Sigma^-$ ,  ${}^1\Delta$ , and  ${}^1\Sigma^+$  ion cores and the relative energies of these electronic states have a profound influence. Table 4 compares the computed energetic minima of the three lowest valence states of the  $\text{FO}^+$  and  $\text{ClO}^+$  ions. The relative energies are CASSCF/MRCI values calculated at the quadruple- $\zeta$  basis level. In  $\text{FO}^+$ , the first two excited states lie almost twice as high in energy relative to the ground state than is the case in  $\text{ClO}^+$ . To identify the core about which any particular Rydberg state is built, we adopted the convention of

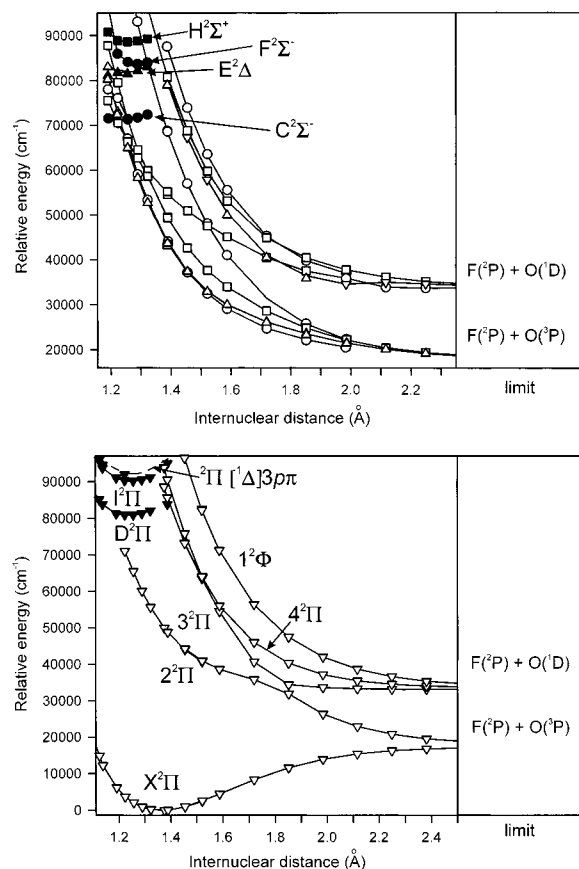


**Figure 3.** CASSCF/MRCI calculations of the potential energy curves for the doublet electronic states of FO. The valence potentials are represented by open symbols, the Rydberg states by solids. Circles denote  $\Sigma^-$  states, squares are  $\Sigma^+$ , triangles are  $\Delta$ , and inverted triangles are  $\Pi$ . The dissociation limits are given in the box on the right. The energies of these asymptotes (relative to the ground state minimum) are given in Table 3. The positions of the asymptote labels on the right are not intended to represent the true dissociation energies. Basis sets used are reported in Table 1. (a, top) The  ${}^2\Sigma^-$ ,  ${}^2\Delta$ , and  ${}^2\Sigma^-$  states. Note that all the valence states of these symmetries are repulsive, just as in ClO. (b, bottom) The calculated  ${}^2\Pi$  states. Three  ${}^2\Pi$  Rydberg states are shown:  $[{}^3\Sigma^-]3p\pi$   $D^2\Pi$ ,  $[{}^3\Sigma^-]3d\pi$   $I^2\Pi$ , and  $[{}^1\Delta]3p\pi$  (unassigned, see text).

**TABLE 4: Relative Energies of the Lowest Three Valence States in the  $\text{FO}^+$  and  $\text{ClO}^+$  Ions<sup>a</sup>**

state	$\text{ClO}^+$		$\text{FO}^+$	
	$r_e/\text{\AA}$	energy of minimum/cm <sup>-1</sup>	$r_e/\text{\AA}$	energy of minimum/cm <sup>-1</sup>
X ${}^3\Sigma^-$	1.4837 <sup>b</sup>	0 <sup>c</sup>	1.2380	0 <sup>d</sup>
a ${}^1\Delta$	1.4878	6 963 (6 961) <sup>28</sup>	1.2389	11 244
b ${}^1\Sigma^+$	1.5027	11 844	1.2515	18 181

<sup>a</sup> These are ab initio values: experimental values are given in parentheses. The basis set used for  $\text{FO}^+$  was AVQZ; for  $\text{ClO}^+$  it was AVQZ + 1. <sup>b</sup> Minimum step size = 0.00005 Å. <sup>c</sup> Absolute energy = -534.392 758 22 hartrees. <sup>d</sup> Absolute energy = -174.264 814 52 hartrees.

identifying the Rydberg states as [ion core]  $n\lambda$ , where the term in the square brackets is the symmetry of the ion core.

As there is no experimental work on the Rydberg states of FO, we label the calculated states in ascending order of energy, starting with the  $C^2\Sigma^-$  Rydberg state, which is also the lowest Rydberg state in  $\text{ClO}^{25}$  and  $\text{BrO}^{26}$ . The doublet Rydberg state orderings are shown in Figure 4 and the energetics of the minima of the states are summarized in Table 5. Because of the expected errors in the ab initio calculations, instead of calculating the

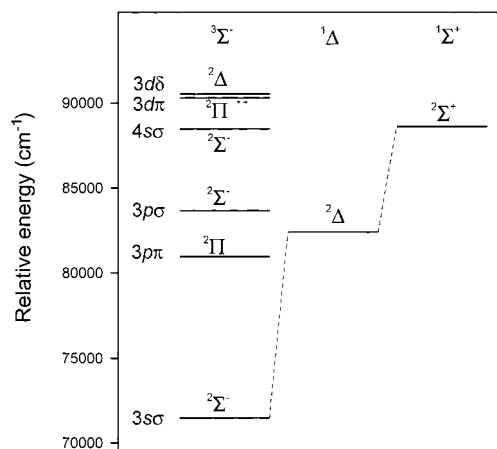


**Figure 4.** Principal configurations of the doublet Rydberg states in FO in terms of a Rydberg molecular orbital (left-hand column) built on a FO<sup>+</sup> ion core (top row).

**TABLE 5: Doublet Rydberg State Energies of FO and Wavelengths Required for (3 + 1) and (2 + 1) REMPI of These States<sup>a</sup>**

state + symmetry <sup>b</sup>	$E(R=1.26 \text{ \AA}) / \text{cm}^{-1}$	$\lambda(3+1)$ REMPI/nm	$\lambda(2+1)$ REMPI/nm
K <sup>2</sup> Σ <sup>-</sup> (3dσ)			
J <sup>2</sup> Δ (3dδ)	90601 <sup>c</sup>	331	221
I <sup>2</sup> Π (3dπ)	90221	333	222
H <sup>2</sup> Σ <sup>+</sup> [ <sup>1</sup> Σ <sup>+</sup> ] (3sσ)	88641	(338) <sup>d,e</sup>	226
G <sup>2</sup> Σ <sup>-</sup> (4sσ)	88621 <sup>f</sup>	338	226
F <sup>2</sup> Σ <sup>-</sup> (3pσ)	83662 <sup>g</sup>	356	238
E <sup>2</sup> Δ [ <sup>1</sup> Δ] (3sσ)	83679	(359) <sup>d,e</sup>	239
D <sup>2</sup> Π (3pπ)	80977	370	247
C <sup>2</sup> Σ <sup>-</sup> (3sσ)	71477	(420) <sup>d,h</sup>	280

<sup>a</sup> The minimum of the X<sup>2</sup>Π state of FO is taken as 1.34 Å and unless specified the minima of the Rydberg states are taken to be 1.26 Å. The total absolute energy calculated for the X<sup>2</sup>Π minimum is -172.695 122 0 hartrees. <sup>b</sup> The ion core is <sup>3</sup>Σ<sup>-</sup> unless stated otherwise. <sup>c</sup> Estimated from the position of the 3dδ orbital in the quartet state calculation. <sup>d</sup> Wavelength in parentheses means that the photon energy is insufficient for a core preserving (3 + 1) REMPI process. <sup>e</sup> Second ionization limit in FO = 111 208 ± 80 cm<sup>-1</sup> = 4 × 350 nm; third ionization limit in FO = 118 063 cm<sup>-1</sup> = 4 × 330 nm. Energies are taken from ref 29. <sup>f</sup> Estimated from the position of the 4sσ orbital in the quartet state calculation. <sup>g</sup> Minimum here approximated as 2.50 bohr (1.33 Å). <sup>h</sup> As the first ionization potential of FO<sup>29</sup> is 103 000 ± 80 cm<sup>-1</sup>, transitions to the C state will not be visible by (3 + 1) REMPI, unlike the situation in ClO.

exact minimum for each Rydberg state, we took the minimum of each state to be approximately the transition energy at  $R = 1.26 \text{ \AA}$  (unless stated otherwise in Table 5), which is close to the minimum energy of the ground state of FO<sup>+</sup>. The energy orderings of the states are rather different than in ClO: for example, in FO the D state is of <sup>2</sup>Π symmetry and not of <sup>2</sup>Δ symmetry because the energy separation of the 3sσ and 3pπ Rydberg orbitals is smaller than the energy required to excite the a<sup>1</sup>Δ-X<sup>3</sup>Σ<sup>-</sup> transition of the FO<sup>+</sup> ion core. It is likely that the Rydberg series of the BrO and IO radicals will also be modified with respect to ClO because of the different relative energies of the molecular Rydberg orbitals and the energy levels of the ion core. Therefore, the state assignments for BrO by Duignan et al.<sup>26</sup> should be treated with some caution.

We do not wish to imply that all the states listed in Table 5 will show resolved spectroscopic structure. A significant difference between FO and ClO is with regard to the lowest C<sup>2</sup>Σ<sup>-</sup> Rydberg state, which was bound in ClO.<sup>25</sup> In FO, however, the lowest repulsive <sup>1</sup>Σ<sup>-</sup> valence state crosses the C<sup>2</sup>Σ<sup>-</sup> Rydberg

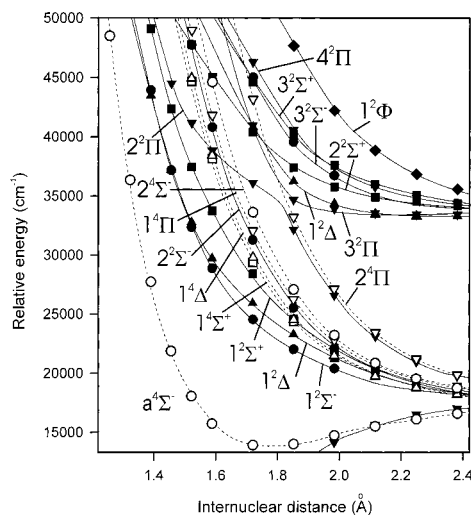


**Figure 5.** Valence electronic states of FO correlating to the two lowest dissociation limits. The quartet state potentials are represented by open symbols and dashed lines, the doublet states by solid symbols and lines. CASSCF/MRCI calculations were performed using the AVQZ basis set. Circles denote Σ<sup>-</sup> states, squares are Σ<sup>+</sup>, triangles are Δ, and inverted triangles are Π. A comparison with the same states in ClO reveals a corresponding pattern of states, except for the A<sup>2</sup>Π state of ClO, which has no bound analogue in FO.

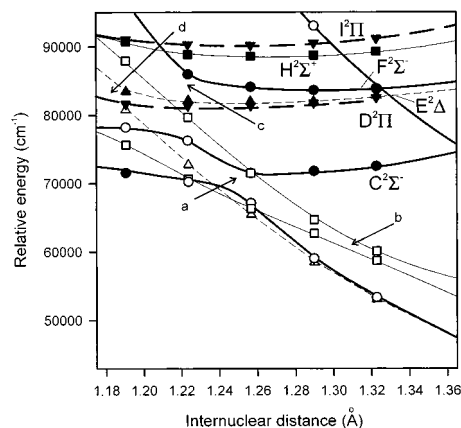


**Figure 6.** Expanded view of the Rydberg region, illustrating the strong valence-Rydberg interactions that may complicate REMPI measurements of these Rydberg states. CASSCF/MRCI calculations were performed using the basis sets in Table 1. Thick solid lines are the <sup>2</sup>Σ<sup>-</sup> adiabatic curves; thin dashed lines are the adiabatic <sup>2</sup>Δ curves; thick dashed curves are <sup>2</sup>Π and thin solid curves are for <sup>2</sup>Σ<sup>+</sup>. Solid and open symbols respectively represent regions of predominantly Rydberg and valence character. The regions marked by arrows a-d denote avoided crossings: a, the C<sup>2</sup>Σ<sup>-</sup>-<sup>1</sup>Σ<sup>-</sup> interaction; b, the <sup>2</sup>Σ<sup>+</sup>-<sup>1</sup>Σ<sup>+</sup> interaction; c, the F<sup>2</sup>Σ<sup>-</sup>-<sup>1</sup>Σ<sup>-</sup> interaction; d, the <sup>1</sup>Δ-E<sup>2</sup>Δ interaction.

state near the potential minimum. Figure 5 shows an expanded view of the low-lying valence states of the FO radical lying in the 13 333 to 50 000 cm<sup>-1</sup> region (one photon absorption between 750 and 200 nm). The predominant configuration of the C<sup>2</sup>Σ<sup>-</sup> Rydberg state is (2420)4sσ, where the numbers in parentheses are the electronic configurations of the pσ, pπ, pπ\*, and pσ\* valence molecular orbitals of the ion core in Mulliken notation.<sup>27</sup> Since the <sup>1</sup>Σ<sup>-</sup> valence state has the configuration (2421), it differs from the Rydberg state by just one spin-orbital, and therefore we expect the C<sup>2</sup>Σ<sup>-</sup> Rydberg state to be heavily predissociated. The Rydberg/valence crossings are highlighted in Figure 6. Indeed, we suspect that all low-lying <sup>2</sup>Σ<sup>-</sup> Rydberg states will be disrupted by this <sup>1</sup>Σ<sup>-</sup> repulsive potential since they all have the same ion core. In addition, the

$^2\Delta$  valence repulsive state (with the same (2421) principal electronic configuration as the  $1^2\Sigma^-$  potential) will also form an avoided crossing with the  $E^2\Delta$  Rydberg state (analogous to the D state in ClO).

The  $H^2\Sigma^+$  Rydberg state has an excited  $1^1\Sigma^+$  ion core, and hence this state will be impossible to access by (3 + 1) REMPI if the ionization step preserves the ion core. A similar argument has been used to account for the weakness or nonappearance of certain states of ClO in (3 + 1) REMPI spectra although they are evident in VUV absorption.<sup>9</sup> To observe the  $H^2\Sigma^+$  Rydberg state via (2 + 1) REMPI, UV of wavelength  $\sim 225$  nm would be necessary. Overall, it appears that the lowest Rydberg  $^2\Sigma^-$ ,  $^2\Sigma^+$ , and  $^2\Delta$  states are rather unsuitable for REMPI detection.

The  $^2\Pi$  Rydberg states are shown in Figure 3b and do not suffer the effects of strong electrostatic predissociation that the other doublet states probably endure because there are no valence  $^2\Pi$  states with the (2421) configuration. The only configuration giving  $^2\Pi$  states that differs from the Rydberg states by one spin-orbital is (2430), and since this is the ground state, predissociation via this state should be negligible, save perhaps at very short internuclear separations. The required wavelength for (3 + 1) REMPI detection of the lowest  $D^2\Pi$  Rydberg ( $\lambda \sim 370$  nm) is difficult to generate with a Nd:YAG-pumped dye laser, though the (2 + 1) scheme at  $\lambda \sim 250$  nm is feasible. (3 + 1) REMPI via the  $I^2\Pi$  state should also be straightforward to implement.

We should also consider the appearance of the low-lying 3d $\delta$  Rydberg orbital in the manifold of doublet Rydberg states, and similarly the 4s $\sigma$  Rydberg orbital. According to the calculations on the quartet states (Figure 2a), the 3d $\delta$  orbital lies above the 3d $\pi$  orbital by  $\sim 380$  cm<sup>-1</sup>, and the 4s $\sigma$  lies  $\sim 1600$  cm<sup>-1</sup> lower. The resulting states are of  $^2\Delta$  and  $^2\Sigma^-$  symmetry, built around the  $^3\Sigma^-$  ion core, and are labeled as the J and G states, respectively. Estimates of the transition energies for the  $J^2\Delta$  and  $G^2\Sigma^-$  states, based on the quartet state calculations, were made in Table 5. We also note that there will be a doublet state based on the 3d $\sigma$  Rydberg orbital, which we label  $K^2\Sigma^-$ , that should be in the vicinity of the  $I^2\Pi$  state, though we are unable to offer a calculated energy minimum as this Rydberg orbital was beyond our calculations. The highest  $^2\Pi$  state in Figure 3b is based on the configuration  $[^1\Delta]3p\pi$ , but the limited active space used in these calculations cannot eliminate the possibility that the  $[^3\Sigma^-]4p\pi$  configuration, which contains the next Rydberg  $\pi$  orbital, lies lower in energy. Therefore, the  $[^1\Delta]3p\pi$  state is excluded from Table 5.

#### 4. Conclusion

Calculations of the energetics of the Rydberg states of FO, which have not been studied experimentally, reveal a different ordering of Rydberg state symmetries than is computed for ClO.

Differences are a consequence of the relative energies of the lowest electronic states of the FO<sup>+</sup> and ClO<sup>+</sup> cores. Detection by REMPI of the  $^2\Pi$  Rydberg states of FO should prove useful in any future kinetic studies involving this radical.

**Acknowledgment.** We thank Prof G. G. Balint-Kurti for use of the Beowulf system at Bristol. I.C.L. thanks the Leverhulme Trust for financial support.

#### References and Notes

- (1) Xie, F. Q.; Xia, Y. X.; Chang, M. Y.; Yuan, D. C.; Wang, Z. Y.; Liu, S. Q.; *Chin. J. Laser* **1991**, *18*, 712.
- (2) Xie, F.; Xia, Y.; Huang, M. *Chem. Phys. Lett.* **1993**, *203*, 598.
- (3) Wayne, R. P.; Poulet, G.; Biggs, P.; Burrows, J. P.; Cox, R. A.; Crutzen, P. J.; Hayman, G. D.; Jenkin, M. E.; Le Bras, G.; Moortgat, G. K.; Platt, U.; Schindler, R. N. "Halogen oxides: radicals, sources and reservoirs in the laboratory and atmosphere"; European Commission Air Pollution Research Report 55, 1995.
- (4) Lane, I. C.; Howie, W. H.; Orr-Ewing, A. J. *Phys. Chem. Chem. Phys.* **1999**, *1*, 3086.
- (5) Ashfold, M. N. R.; Clement, S. G.; Howe, J. D.; Western, C. M. J. *Chem. Soc. Faraday Trans.* **1993**, *89*, 1153.
- (6) Roos, B. *Adv. Chem. Phys.* **1987**, *69*, 399.
- (7) Knowles, P. J.; Werner, H. J. *Chem. Phys. Lett.* **1985**, *115*, 259. Werner, H. J.; Knowles, P. J. *J. Chem. Phys.* **1985**, *82*, 5053.
- (8) Werner, H. J.; Knowles, P. J. *J. Chem. Phys.* **1988**, *89*, 5803. Knowles, P. J.; Werner, H. J. *Chem. Phys. Lett.* **1988**, *145*, 514.
- (9) Lane, I. C.; Orr-Ewing, A. J. *Mol. Phys.* **2000**, *98*, 793.
- (10) Kendall, R. A.; Dunning, Jr. T. H.; Harrison, R. J. *J. Chem. Phys.* **1992**, *96*, 6796. Woon, D. E.; Dunning Jr., T. H. *J. Chem. Phys.* **1994**, *100*, 2975.
- (11) Martin, J. M. L.; Uzan, O. *Chem. Phys. Lett.* **1998**, *282*, 16.
- (12) van Mourik, T.; Wilson, A. K.; Peterson, K. A.; Woon, D. E.; Dunning, T. H. *Adv. Quantum Chem.* **1998**, *31*, 105.
- (13) MOLPRO 98.1 is a package of ab initio programs written by: Werner H. J.; Knowles P. J., with contributions of: Almløf, J.; Amos, R. D.; Berning, A.; Cooper, D. L.; O'Deeagan, M. J.; Dobbyn, A. J.; Eckert, F.; Elbert, S. T.; Hampel, A. C.; Lindl, R.; Lloyd, A. W.; Meyer, W.; Mura, M. E.; Nicklass, A.; Peterson, K. A.; Pitzer, R. M.; Pulay, P.; Schutz, M.; Stoll, H.; Stone, A.; Taylor, P. R.; Thorsteinsson, T.
- (14) Langhoff, S. R.; Davidson, E. R. *Int. J. Quantum Chem.* **1974**, *8*, 61.
- (15) Lawley, K. P.; Donovan, R. J. *J. Chem. Soc., Faraday Trans.* **1993**, *89*, 1885.
- (16) Huang, M. B. *Chin. Chem. Lett.* **1996**, *7*, 475.
- (17) Moore, C. E. *Atomic Energy Levels*; Natl. Bur. Stand. (U.S.) Circ. No. 35; U.S. GPO: Washington, DC, 1971; Vol. I.
- (18) The NIST webpage can be found at <http://physics.nist.gov/cgi-bin/AtData>.
- (19) Kelly, R. L. *J. Phys. Chem. Ref. Data* **1987**, *16* (S1), 1.
- (20) Blondel, C. *Phys. Scr.* **1995**, *T58*, 31.
- (21) Blondel, C.; Cacciani, P.; Delsart, C.; Trainham, R. *Phys. Rev. A* **1989**, *40*, 3698.
- (22) Dressler, K.; Miescher, E. *Astrophys. J.* **1965**, *141*, 1266.
- (23) Miescher, E. *J. Mol. Spectrosc.* **1966**, *20*, 130.
- (24) Jungen, Ch. *J. Chem. Phys.* **1970**, *53*, 4168.
- (25) Coxon, J. A. *Can. J. Phys.* **1979**, *57*, 1538.
- (26) Duignan, M. T.; Hudgens, J. W. *J. Chem. Phys.* **1985**, *82*, 4426.
- (27) Mulliken, R. J. *J. Chem. Phys.* **1971**, *55*, 288.
- (28) Wales, N. P. L.; Buma, W. J.; de Lange, C. A. *Chem. Phys. Lett.* **1996**, *259*, 213.
- (29) Dyke, J. M.; Jonathan, N.; Mills, J. D.; Morris, A. *Mol. Phys.* **1980**, *40*, 1177.